

Received: 2019.10.13

Accepted: 2020.01.20

Available online: 2020.02.25

Published: 2020.04.30

# Carbon Monoxide Inhibits the Expression of Proteins Associated with Intestinal Mucosal Pyroptosis in a Rat Model of Sepsis Induced by Cecal Ligation and Puncture

Authors' Contribution:  
Study Design A  
Data Collection B  
Statistical Analysis C  
Data Interpretation D  
Manuscript Preparation E  
Literature Search F  
Funds Collection G

ABCDEF 1 **Hongzhou Wang\***  
BC 2 **Shunwen Zhang\***  
AF 3 **Haijun Zhao\***  
C 2 **Huiyuan Qin**  
AD 3 **Jie Zhang**  
FG 3 **Jiangtao Dong**  
G 1 **Hui Zhang**  
AE 1 **Xiaoling Liu**  
BF 1 **Zhengyong Zhao**  
BF 3 **Yanheng Zhao**  
BF 1 **Meng Shao**  
AEF 1 **Fang Wu**  
AEFG 1 **Wanjiang Zhang**

1 Department of Pathophysiology, Shihezi University School of Medicine and The Key Laboratory of Xinjiang Endemic and Ethnic Diseases, Shihezi, Xinjiang, P.R. China  
2 The First School of Clinical Medicine, Nanjing Medical University, Nanjing, Jiangsu, P.R. China  
3 The First Affiliated Hospital of the Medical College, Shihezi University, Shihezi, Xinjiang, P.R. China

\* Hongzhou Wang, Shunwen Zhang and Haijun Zhao contributed equally

Wanjiang Zhang, e-mail: [zwj1117@126.com](mailto:zwj1117@126.com), Fang Wu, e-mail: [xjwufang@126.com](mailto:xjwufang@126.com)

**Corresponding Authors:**  
**Source of support:**

This study was funded by the National Natural Science Foundation Project (Grant No. U1803127), the Xinjiang Uygur Autonomous Region graduate student innovation project (Grant No. XJGR12016042), and the Key Science and Technology Research Projects in Key Areas of the Corps in 2018 (Grant No. 2018AB019)

**Background:** Carbon monoxide (CO) has anti-inflammatory effects and protects the intestinal mucosal barrier in sepsis. Pyroptosis, or cell death associated with sepsis, is mediated by caspase-1 activation. This study aimed to investigate the role of CO on the expression of proteins associated with intestinal mucosal pyroptosis in a rat model of sepsis induced by cecal ligation and puncture (CLP).


**Material/Methods:** The rat model of sepsis was developed using CLP. Male Sprague-Dawley rats (n=120) were divided into six study groups: the sham group (n=20); the CLP group (n=20); the hemin group (treated with ferric chloride and heme) (n=20); the zinc protoporphyrin IX (ZnPPiX) group (n=20); the CO-releasing molecule 2 (CORM-2) group (n=20); and the inactive CORM-2 (iCORM-2) group (n=20). Hemin and CORM-2 were CO donors, and ZnPPiX was a CO inhibitor. In the six groups, the seven-day survival curves, the fluorescein isothiocyanate (FITC)-labeled dextran 4000 Da (FD-4) permeability assay, levels of intestinal pyroptosis proteins caspase-1, caspase-11, and gasdermin D (GSDMD) were measured by confocal fluorescence microscopy. Proinflammatory cytokines interleukin (IL)-18, IL-1 $\beta$ , and high mobility group box protein 1 (HMGB1) were measured by Western blot and enzyme-linked immunosorbent assay (ELISA).

**Results:** CO reduced the mortality rate in rats with sepsis and reduced intestinal mucosal permeability and mucosal damage. CO also reduced the expression levels of IL-18, IL-1 $\beta$ , and HMGB1, and reduced pyroptosis by preventing the cleavage of caspase-1 and caspase-11.

**Conclusions:** In a rat model of sepsis induced by CLP, CO had a protective role by inhibiting intestinal mucosal pyroptosis.

**MeSH Keywords:** **Carbon Monoxide • Cell Death • Intestinal Mucosa • Sepsis**

**Full-text PDF:** <https://www.medscimonit.com/abstract/index/idArt/920668>

 4339

 1

 8

 59



## Background

Sepsis involves a systematic inflammatory reaction following infection that can affect tissues and organs [1]. Previous studies have shown that intestinal injury is present during systemic sepsis, which affects the protective barrier functions of the intestinal mucosa [2–4]. The intestinal epithelium not only acts as a passive barrier but also has a role in antigen-presentation to adjacent lymphoid tissue as part of the intestinal mucosal immune response [5]. Carbon monoxide (CO) gas has been shown to have anti-inflammatory effects on the intestinal mucosa and the lungs in experiential models [6,7]. The endogenous CO donor, hemin, and the exogenous CO donor, CO-releasing molecule 2 (CORM-2), have previously been investigated in research studies on sepsis [6,7]. However, the mechanisms of the effects of CO in sepsis remain unclear.

Pyroptosis, or cell death associated with sepsis, is mediated by caspase-1 activation and has previously been shown to be an important factor associated with cell death in inflammation [8,9]. Increased cell pyroptosis plays a critical role in the development of sepsis and septic shock [10–12]. In a previous study, Wu et al. showed that CO treatment reduced radiation-induced intestinal injury in patients with cancer and protected the intestinal cells by reducing pyroptosis [13]. Zhang et al. reported that CORM-3 suppressed the activation of the NLRP3 inflammasome in myocardial dysfunction due to sepsis [14]. Wang et al. previously showed that CORM-2 reduced the activity of the NLRP3 inflammasome in sepsis-induced acute kidney injury [15]. The NLRP3 inflammasome is one of the key factors involved in pyroptosis [16].

Therefore, this study aimed to investigate the role of CO on the expression of proteins associated with intestinal mucosal pyroptosis in a rat model of sepsis induced by cecal ligation and puncture (CLP).

## Material and Methods

### Reagents

Hemin (no. 51280), zinc protoporphyrin IX (ZnPPiX) (no.282820), Carbon monoxide (CO)-releasing molecule 2 (CORM-2) (no.288144), and dextran 4000 Da (FD-4) (46944) were obtained from Sigma-Aldrich (St. Louis, MO, USA). Dimethylsulfoxide (DMSO) (D3870), phosphate buffer saline (PBS) (P1020), and 4% paraformaldehyde (P1110) were obtained from Beijing Solarbio Science & Technology Co. Ltd. (Beijing, China). CORM-2 was dissolved in 0.5% of DMSO at 37°C in a sterile incubator for 24 h, and the resulting inactive CORM-2 (iCORM-2) was used as a negative control. Antibodies used were to caspase-1 (ab1872; Abcam, Shanghai, China), gasdermin D (GSDMD) (ab219800;

Abcam, Shanghai, China), and caspase-11 p20 (sc-374615; Santa Cruz Biotechnology, Texas, USA). Enzyme-linked immunosorbent assay (ELISA) kits included rat tumor necrosis factor- $\alpha$  (TNF- $\alpha$ ) (E-EL-R0019c), rat interleukin-1 $\beta$  (IL-1 $\beta$ ) (E-EL-R0012c), rat IL-18 (E-EL-R0567c), and rat high mobility group box protein 1 (HMGB1) (E-EL-R0505c) (Elabscience Biotechnology Co., Ltd., Wuhan, China). The ELISA results were analyzed using a Multiskan Spectrum spectrophotometer (ThermoFisher Scientific, Waltham, MA, USA).

### The rat model of sepsis induced by cecal ligation and puncture (CLP)

The animal experiments were approved by the Animal Care Committee of the First Affiliated Hospital Medical College, Shihezi University (Approval No. A2017-165-01). The experimental protocols followed the guidelines of the Animal Care Committee. The study included 120 specific pathogen-free (SPF) male Sprague-Dawley rats between 8–10 weeks of age, weighing 180–200 g. The rats were obtained from the Laboratory Animal Center of Xinjiang Medical University, Urumqi, China (animal license no. XJYK0011, 2011).

Male Sprague-Dawley rats (n=120) were divided into six study groups: the sham group (n=20); the CLP group (n=20); the hemin group (treated with ferric chloride and heme) (n=20); the zinc protoporphyrin IX (ZnPPiX) group (n=20); the CO-releasing molecule 2 (CORM-2) group (n=20); and the inactive CORM-2 (iCORM-2) group (n=20). A total of 10, 5, and 5 rats were used for the 7-day survival analysis, the fluorescein isothiocyanate (FITC)-labeled dextran 4000 Da (FD-4) permeability assay, and the cytokine expression study, respectively.

The rats were housed in individual cages at a constant temperature of 22 $\pm$ 1°C with a 12-hourly light and dark cycle and were acclimated for 3 days before the study began. The rats were given food and water *ad libitum* and then fasted for 12 hours before the study commenced. A total of 10, 5, and 5 rats were used for the 7-day survival analysis, the fluorescein isothiocyanate (FITC)-labeled dextran 4000 Da (FD-4) permeability assay, and cytokine expression in the study groups, respectively.

### Treatments used

All rats were anesthetized with 1% pentobarbital (30 mg/kg) (Merck KGaA, Darmstadt, Germany), which was given intraperitoneally. The sepsis model was constructed using cecal ligation and puncture in all but the sham group. Hemin, ZnPPiX, and CORM-2 were dissolved and diluted by using 0.5% DMSO, respectively, the cecum was punctured twice with a 21-gauge needle and ligated, and the bowel content was squeezed out to induce abdominal infection.

After the CLP surgery, the rats in the sham group, the CLP group, the hemin group, the ZnPPIX group, the CORM-2 group, and the iCORM-2 group were treated intraperitoneally with 0.5 ml 0.5% DMSO, 0.5 ml 0.5% DMSO, 8 mg/kg hemin+0.5 ml 0.5% DMSO, 8 mg/kg ZnPPIX+0.5 ml 0.5% DMSO, 8 mg/kg CORM-2+0.5 ml 0.5% DMSO and 8 mg/kg inactive CORM-2+0.5 ml 0.5% DMSO, respectively. At 18 h after the CLP surgery, rats in each group were treated with dextran 4000 Da (FD-4) solution dissolved in PBS (PH 7.4) (20 mg/ml, 20 mg/200 g) by gavage. Survival curve analysis was performed for each group.

### Sample collection and examination

At 24 h after the CLP surgery, the rats treated with FD-4 solution were anesthetized, and 2 ml of blood was collected through the portal vein. The blood samples were centrifuged for 15 min at 3000×g at 4°C to measure the FD-4 concentration in the blood. For the other rats, 2 ml of blood samples from the abdominal aorta were centrifuged at 3,000×g for 15 min to obtain the serum for the measurement of serum cytokine levels.

The rat intestinal tissue was harvested (approximately 8 cm) in cold PBS. Part of the intestinal tissue was crushed in a mortar and the tissue fluid was centrifuged twice at 12,000×g for 20 min per time at 4°C. The tissue homogenate was used to detect the proteins by Western blot. The remaining tissue was fixed in 4% paraformaldehyde (Solarbio, Beijing, China) for histological examination. The serum and intestinal tissue fluid were used to measure the levels of IL-1 $\beta$ , IL-18, HMGB-1, and TNF- $\alpha$  by ELISA.

Survival analysis was performed for 10 rats per group in the sham, CLP, hemin, ZnPPIX, CORM-2, and iCORM-2 groups. The survival status of the rats was recorded every 24 h until the seventh day.

### The fluorescein isothiocyanate (FITC)-labeled dextran 4000 Da (FD-4) permeability assay

Blood (2 ml) was collected from the portal vein six hours after the administration of dextran 4000 Da (FD-4), and centrifuged at 3000×g for 15 min at 4°C. The content of FD-4 was measured using a Varioskan Flash multimode microplate reader (ThermoFisher Scientific, Waltham, MA, USA) at a 490 nm emission wavelength and a 520 nm excitation wavelength.

### Histology and the scoring of intestinal necrosis and inflammation

The intestinal tissue samples were fixed in 4% paraformaldehyde for 48 h at 20°C. Tissues were sectioned at 4  $\mu$ m onto glass slides and stained with hematoxylin and eosin (H&E). The tissue sections were examined by light microscopy at a

magnification of  $\times$ 100. The histological scoring system for intestinal necrosis and inflammation was used, as described by Chiu et al. in 1970 [17], which combined the histological, morphological, and hemodynamic tissue changes. The scores used were as follows: 0, normal mucosa; 1, mucosal degeneration with an increased subepithelial space; 2, raised intestinal villous epithelium with further increase in the subepithelial space; 3, intestinal villous epithelium detachment; 4, intestinal villous epithelium loss to leave the lamina propria; 5, severe degeneration and disintegration of the lamina propria with ulceration [17]. Five fields of view per group were evaluated independently by two pathologists, according to the previously described scoring system [17].

### Western blot

The protein content of the intestinal tissue homogenate supernatant was detected by the bicinchoninic acid (BCA) protein assay using RIPA buffer and phenylmethyl sulfonyl fluoride (PMSF) (Solarbio Technology Co. Ltd., Beijing, China). The solution was mixed with loading buffer (Beyotime, Shanghai, China) and boiled for 10 min. The samples underwent 12% sodium dodecyl sulfate-polyacrylamide gel electrophoresis (SDS-PAGE) with 250  $\mu$ g of protein in each lane. The protein was transferred to polyvinylidene fluoride (PVDF) membranes (ThermoFisher Scientific, Waltham, MA, USA). After blocking with 5% dried skimmed milk powder for 2 h at room temperature, the membranes were incubated in the primary antibodies. The primary antibodies were to caspase-1 (1: 1,000) (ab1872; Abcam, Shanghai, China), caspase-11 (1: 500) (sc-374615; Santa Cruz Biotechnology, Texas, USA), GSDMD (1: 1000) (ab219800; Abcam, Shanghai, China), and  $\beta$ -actin (1: 5000) (TA-09, Santa Cruz Biotechnology, Texas, USA). The primary antibodies were incubated on the membranes at 4°C overnight. The horse-radish peroxidase (HRP)-conjugated secondary antibodies were incubated on the membranes for 2 h at room temperature and included goat anti-rabbit antibody (1: 20,000) (ZB2301; Zhongshan Golden Bridge Biotechnology Co., Ltd, Beijing, China). The membranes were washed and developed using a Beyo ECL Plus, P0018 enhanced chemiluminescence (ECL) system (Beyotime, Shanghai, China). The intensity of the bands was quantified by using ImageJ software version 1.42i (National Institutes of Health, Bethesda, MD, USA). The ratio of the target proteins to the  $\beta$ -actin bands was calculated.

### Immunofluorescence staining

The tissue sections of rat intestine were incubated with primary antibodies to caspase-1 (1: 200) (ab1872; Abcam, Shanghai, China) and caspase-11 (1: 200) (sc-374615; Santa Cruz Biotechnology, Texas, USA) at 4°C overnight. A fluorescein-conjugated secondary goat anti-rabbit antibody (ZF-0311), goat anti-mouse antibody (1: 100) (ZF-0312) was incubated for 2 h

at room temperature. The nuclei were stained with propidium iodide (PI) (Sigma-Aldrich, St. Louis, MO, USA), and the tissue was examined under a Zeiss LSM 510 laser confocal scanning microscope (Carl Zeiss AG, Munich, Germany). The fluorescence intensity was quantified by using ImageJ version 1.42I software (National Institutes of Health, Bethesda, MD, USA).

### Measurement of serum and intestinal tissue cytokine levels

Blood (2 ml) was collected from the abdominal aorta at 24 h after intraperitoneal injection using 0.5 ml of 0.5% DMSO, 0.5 ml of 0.5% DMSO, 8 mg/kg of hemin+0.5 ml of 0.5% DMSO, 8 mg/kg ZnPPiX+0.5 ml of 0.5% DMSO, 8 mg/kg CORM-2+0.5 ml of 0.5% DMSO and 8 mg/kg of inactive CORM-2+0.5 ml of 0.5% DMSO, respectively. Blood was centrifuged at 3000×g for 15 min at 4°C using a 5427R super-centrifuge (Eppendorf, Hamburg, Germany), and the supernatant was retained. The levels of the inflammatory cytokines, TNF- $\alpha$ , IL-1 $\beta$ , IL-18, and HMGB1 in the serum and intestinal tissue homogenates, were measured using ELISA kits, according to manufacturer's instructions (Elabscience Biotechnology Co., Ltd., Wuhan, China). The ELISA results were analyzed using a Multiskan Spectrum spectrophotometer (ThermoFisher Scientific, Waltham, MA, USA).

### Statistical analysis

Data were analyzed using SPSS version 22.0 software (IBM Corp., Armonk, NY, USA). The median survival time was recorded for the rat groups, and the difference in survival between the experimental groups was analyzed by using the Kaplan-Meier log-rank test. Quantitative data were expressed as the mean±standard error (SE) and compared using one-way analysis of variance (ANOVA) when the data were normally distributed. The least significant difference (LSD) post hoc test was used to compare the differences between the two groups. The Kruskal-Wallis non-parametric test was used to compare differences between multiple groups, followed by Bonferroni's post hoc test. A P-value <0.05 was considered to be statistically significant.

## Results

### Carbon monoxide (CO) increased the survival rate in the rat model of sepsis induced by cecal ligation and puncture (CLP)

Male Sprague-Dawley rats (n=120) were divided into six study groups: the sham group (n=20); the CLP group (n=20); the hemin group (treated with ferric chloride and heme) (n=20); the zinc protoporphyrin IX (ZnPPiX) group (n=20);

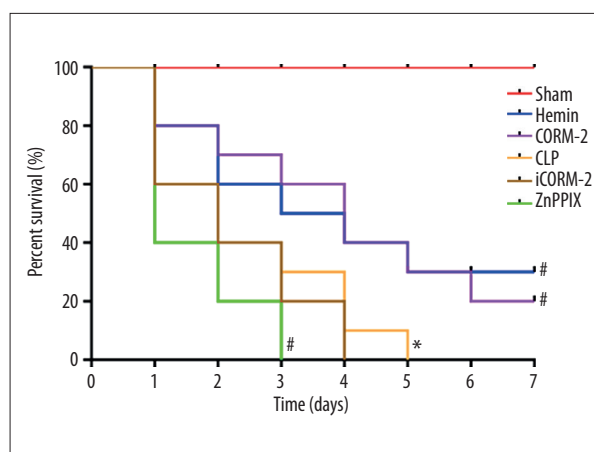


**Figure 1.** The effect of carbon monoxide (CO) on the survival rate in the rat model of sepsis induced by cecal ligation and puncture (CLP). Rats from each study group (n=10) were assessed to determine the 7-day survival rate. The Kaplan-Meier survival curves are shown. Male Sprague-Dawley rats (n=120) were divided into six study groups: the sham group; the CLP group; the hemin group (treated with ferric chloride and heme); the zinc protoporphyrin IX (ZnPPiX) group; the CO-releasing molecule 2 (CORM-2) group; and the inactive CORM-2 (iCORM-2) group. FD-4 – fluorescein isothiocyanate-labeled dextran 3000–4000 kDa; CLP – cecal ligation and puncture; CORM-2 – CO-releasing molecule 2; Hemin – ferric chloride heme; ZnPPiX – zinc protoporphyrin IX; iCORM-2 – inactive CORM-2.

the CO-releasing molecule 2 (CORM-2) group (n=20); and the inactive CORM-2 (iCORM-2) group (n=20).

Hemin and CORM-2 treatment were associated with reduced mortality in the rats in the CLP model, whereas ZnPPiX treatment was associated with increased mortality compared with the CLP group. The iCORM-2 group had no significant change in mortality. On the first day, the survival rate of the sham group, the hemin group, and the CORM-2 group was 100%, 80%, and 80%, respectively. The survival rate of the CLP group and the ZnPPiX group was significantly reduced to 60% and 40%, respectively (Figure 1). On the third day, the rats in the ZnPPiX group were all dead, and the survival rate of rats in the CLP group was 30%, and the survival rates in the hemin and the CORM-2 groups was 50% and 60% respectively (Figure 1). On the fourth and fifth days, the rats in the iCORM-2 and CLP groups had died. On the seventh day, the survival rate in the hemin group and the CORM-2 group was 30% and 20%, respectively. The median survival time in the study groups was 7 days, 2 days, 3 days, 1 day, 4 days and 2 days, respectively (Figure 1).

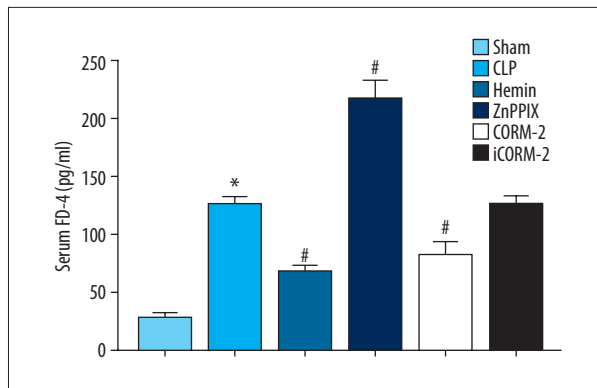


**Figure 2.** The serum dextran 4000 Da (FD-4) levels in the study groups in the rat model of sepsis induced by cecal ligation and puncture (CLP). Male Sprague-Dawley rats (n=120) were divided into six study groups: the sham group; the CLP group; the hemin group (treated with ferric chloride and heme); the zinc protoporphyrin IX (ZnPPIX) group; the CO-releasing molecule 2 (CORM-2) group; and the inactive CORM-2 (iCORM-2) group. The bars represent the mean±standard error (SE) (n=3~5). \* P<0.05 versus the sham group. # P<0.05 versus the CLP group. FD-4 – fluorescein isothiocyanate-labeled dextran 3000~4000 kDa; CLP – cecal ligation and puncture; CORM-2 – CO-releasing molecule 2; Hemin – ferric chloride heme; ZnPPIX – zinc protoporphyrin IX; iCORM-2 – inactive CORM-2.

### CO improved the intestinal mucosa permeability in the rat CLP model of sepsis

The normal intestinal mucosa does not absorb dextran 4000 Da (FD-4), and so FD-4 serum concentrations were measured to assess the changes in intestinal mucosal permeability and the damage to the intestinal mucosa in the rats in the CLP model of sepsis. As shown in Figure 2 and Table 1, the FD-4 levels in the CLP group (125.6±1.57 pg/ml) were significantly higher when compared with the sham group (28.16±2.60 pg/ml) (P<0.05). Dextran 4000 Da (FD-4) in the hemin group (67.66±3.11 pg/ml) and the CORM-2 group (81.48±13.10 pg/ml) reduced the level of serum FD-4 compared with that of the CLP group (P<0.05). However, ZnPPIX (214.47 ± 9.38 pg/ml) increased the level of dextran 4000 Da (FD-4) and increased intestinal tissue injury compared with the CLP group (P<0.05). The iCORM-2 group (120.4±1.70 pg/ml) showed no significant changes compared with the CLP group (P>0.05) (Figure 2, Table.1).

### CO reduced the damage to the intestinal mucosa in the rat CLP model of sepsis

The histological scoring system was used to analyze the degree of intestinal mucosal damage, and the histological changes are shown in Figure 3. As shown in Figure 3A, intact intestinal mucosa was observed in the sham group, and mucosal injury

**Table 1.** Serum cytokines, FD-4 level and intestinal cytokines levels at 24 h after CLP.

Variables	IL-1β (pg/ml)	IL-18 (pg/ml)	HMGB1 (pg/ml)	TNF-α (pg/ml)	FD-4 (pg/ml)
<b>Serum indexes changes after 24 h after CLP</b>					
Sham (n=5)	130.05±4.6	258.22±1.52	430.78±1.76	726.95±14.83	28.16±2.60
CLP (n=5)	256.02±3.32*	352.1±6.18*	1476.48±4.25*	952.81±12.45*	125.6±1.57*
Hemin (n=5)	128.32±4.69#	294.64±3.41#	524.41±2.03#	848.19±13.41#	67.66±3.11#
ZnPPIX (n=5)	305.39±3.09#	370.95±6.18#	2186.0±5.66#	1111±11.31#	214.4±9.38#
CORM-2 (n=5)	144.3±4.40#	270.09±0.52#	1163.13±3.58#	714.47±15#	81.4±13.10#
iCORM-2 (n=5)	230.15±3.47	340.73±5.56	1733.66±4.78	942.37±12.54	120.4±1.7
<b>Intestinal tissue cytokines levels at 24 h after CLP</b>					
Sham (n=5)	165.73±10.55	199.48±7.95	117.57±9.36	259.49±15.84	
CLP (n=5)	888.4±50.93*	455.3±8.58*	251.93±29.2*	452.89±15.93*	
Hemin (n=5)	721.9±57.87#	331.1±12.11#	154.1±7.82#	341.99±11.32#	
ZnPPIX (n=5)	1143.1±47.23#	567.17±7.26#	537.27±22.32#	561.49±16.01#	
CORM-2 (n=5)	637.48±60.55#	354.1±8.6#	192.79±17.76#	304.57±10.23#	
iCORM-2 (n=5)	828.6±52.74	468.6±4.53	260.0±17.65	452.83±19.86	

Data are shown as mean±SE. \* P<0.05 versus Sham group. # P<0.05 versus CLP group. FD-4 – fluorescein isothiocyanate-labeled dextran 3000~4000 kDa; CLP – cecal ligation and puncture; CORM-2 – CO releasing molecule 2; iCORM-2 – inactive CORM-2; Hemin – ferric chloride heme; ZnPPIX – zinc protoporphyrin IX; TNF-α – tumor necrosis factor alpha; IL-1β – interleukin-1β; IL-18 – interleukin-18; HMGB1 – high mobility group box protein 1.

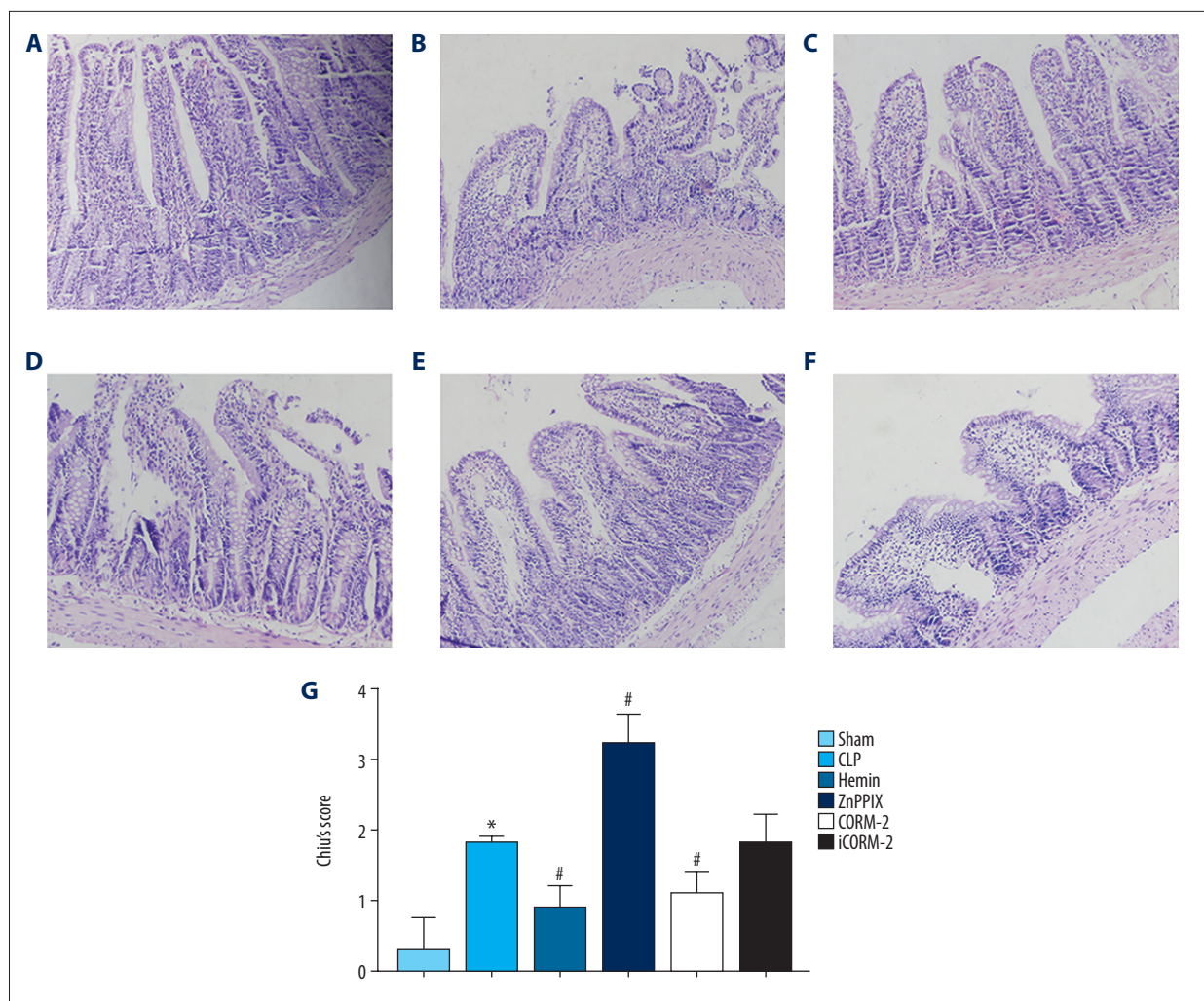


**Figure 3.** Photomicrographs of the histology stained with hematoxylin and eosin (H&E) of the intestinal tissue in the study groups in the rat model of sepsis induced by cecal ligation and puncture (CLP). Carbon monoxide (CO) protected the intestinal mucosa from damage associated with cecal ligation and puncture (CLP)-induced sepsis. Representative photomicrographs of the histology of the rat intestine tissue stained with hematoxylin and eosin (H&E). Original magnification,  $\times 100$ . Male Sprague-Dawley rats ( $n=120$ ) were divided into six study groups: (A) the sham group, (B) the CLP group, (C) the hemin group (treated with ferric chloride and heme), (D) the zinc protoporphyrin IX (ZnPPIX) group, (E) the CO-releasing molecule 2 (CORM-2) group, and (F) the inactive CORM-2 (iCORM-2) group. (G) The histology scores of the different groups. The bars represent the mean  $\pm$  standard error (SE) ( $n=3-5$ ). \*  $P<0.05$  versus the sham group. #  $P<0.05$  versus the CLP group. FD-4 – fluorescein isothiocyanate-labeled dextran 3000–4000 KDa; CLP – cecal ligation and puncture; CORM-2 – CO-releasing molecule 2; Hemin – ferric chloride heme; ZnPPIX – zinc protoporphyrin IX; iCORM-2 – inactive CORM-2.

was observed in the CLP group (Figure 3B) and the iCORM-2 group (Figure 3F). Severe intestinal mucosal injury was observed in the ZnPPIX group (Figure 3D). The intestinal mucosal damage in the hemin group (Figure 3C) and the CORM-2 group (Figure 3E) was less than the CLP group (Figure 3B). Figure 3G shows that the ZnPPIX group had the highest scores ( $3.2 \pm 0.2$ ) and the hemin group ( $0.9 \pm 0.57$ ) and CORM-2 group ( $1.1 \pm 0.18$ ) scores were significantly reduced compared with the CLP group ( $1.8 \pm 0.25$ ). The iCORM-2 score was lower than the CLP group, but the difference did not reach statistical significance (Figure 3G).

### CO reduced the levels of proinflammatory cytokines in the rat CLP model of sepsis

Figures 4 and 5, and Table 1 show the levels of TNF- $\alpha$ , IL-18, IL-1 $\beta$ , and HMGB1 in the serum and intestinal tissue homogenates in the rat study groups. The levels of TNF- $\alpha$ , IL-18, IL-1 $\beta$ , and HMGB1 in the serum and intestinal homogenates were increased in the CLP rats compared with the sham group ( $P<0.05$ ). However, the levels in the ZnPPIX group were significantly increased when compared with the CLP group and other groups ( $P<0.05$ ). Hemin or CORM-2 significantly reduced the levels of

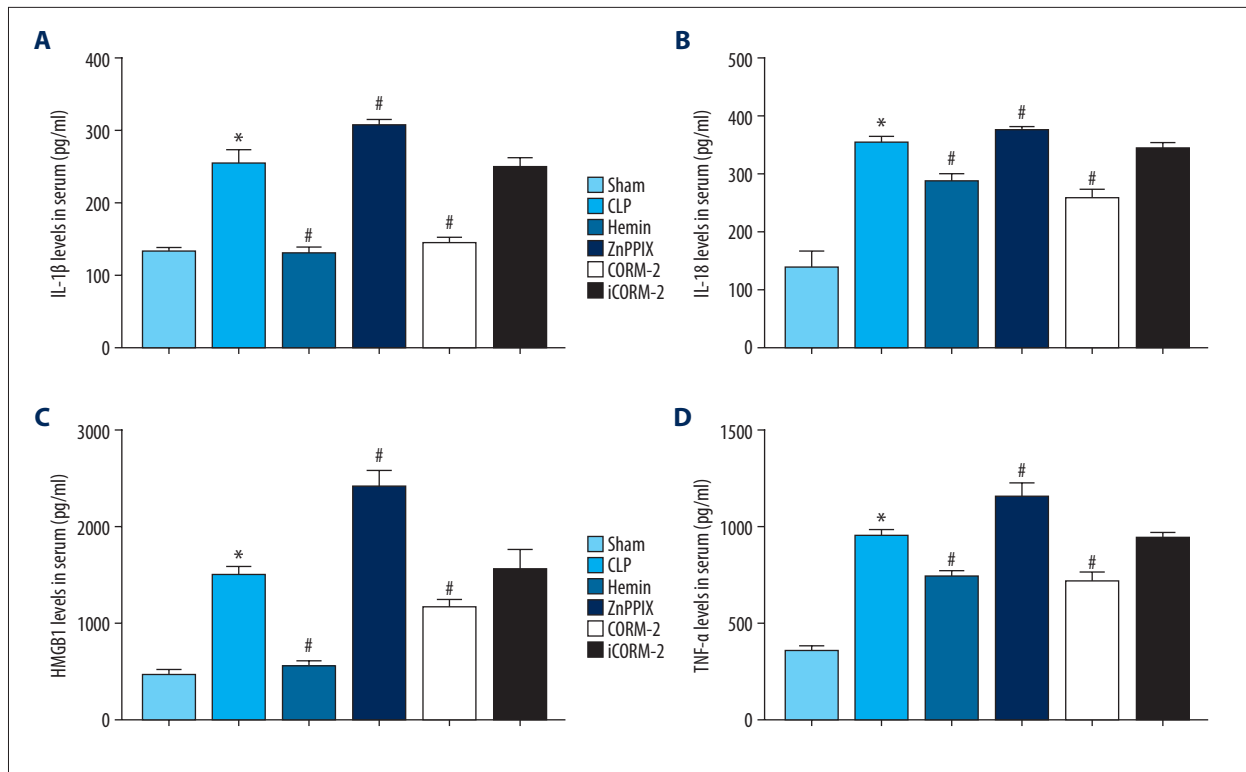


**Figure 4. (A–D)** The serum levels of proinflammatory cytokines in the study groups in the rat model of sepsis induced by cecal ligation and puncture (CLP). Male Sprague-Dawley rats (n=120) were divided into six study groups: the sham group, the CLP group, the hemin group (treated with ferric chloride and heme), the zinc protoporphyrin IX (ZnPPIX) group, the CO-releasing molecule 2 (CORM-2) group, and the inactive CORM-2 (iCORM-2) group. The bars represent the mean±standard error (SE) (n=3–5), \* P<0.05 versus the sham group. # P<0.05 versus the CLP group. FD-4 – fluorescein isothiocyanate-labeled dextran 3000–4000 KDa; CLP – cecal ligation and puncture; CORM-2 – CO-releasing molecule 2; Hemin – ferric chloride heme; ZnPPIX – zinc protoporphyrin IX; iCORM-2 – inactive CORM-2.

TNF- $\alpha$ , IL-18, IL-1 $\beta$ , and HMGB1 compared with the CLP and ZnPPIX groups (P<0.05), and there was no significant difference between the CORM-2 and the iCORM-2 groups (P>0.05).

### CO reduced upregulation of pyroptosis proteins in the rat CLP model of sepsis

Western blot and immunofluorescence analysis methods were used to analyze pyroptosis-associated molecules of the mid ileum. The expression of pro-caspase-1, pro-caspase-11, caspase-1 p20, caspase-11 p20 and GSDMD in the intestinal mucosa were significantly upregulated in the CLP group compared with the sham group (P<0.05, Figure 6). However, the expression of pro-caspase-1, pro-caspase-11, caspase-1 p20, caspase-11 p20, and GSDMD increased in the ZnPPIX group compared with the CLP group (P<0.05) (Figure 6). Detection of caspase-1 and caspase-11 by laser confocal microscopy demonstrated that caspase-1 and caspase-11 expression were upregulated in the CLP group compared with the sham group (P<0.05) and showed green fluorescence using the confocal microscope (Figures 7, 8). Hemin and CORM-2 treatment

significantly reduced the expression of caspase-1 and caspase-11 compared with the CLP group and the ZnPPIX group, and significantly upregulated the expression of caspase-1 and caspase-11 (P<0.05) (Figures 7, 8). These results indicated that CO regulated the caspase-1 related canonical and caspase-11 related noncanonical pathway of pyroptosis in the rat model of sepsis induced by CLP.

### Discussion

Although there have been several reported studies on the pathophysiology of sepsis, the condition remains difficult to control and treat [1]. Recently, the association between systemic sepsis and the loss of the intestinal barrier function has become an area of interest in clinical and preclinical research [18]. The dysfunction of the intestinal barrier increases the severity and progression of sepsis [19,20]. Therefore, the intestinal tract should be regarded as participating in the systemic inflammatory response in sepsis [21,22].

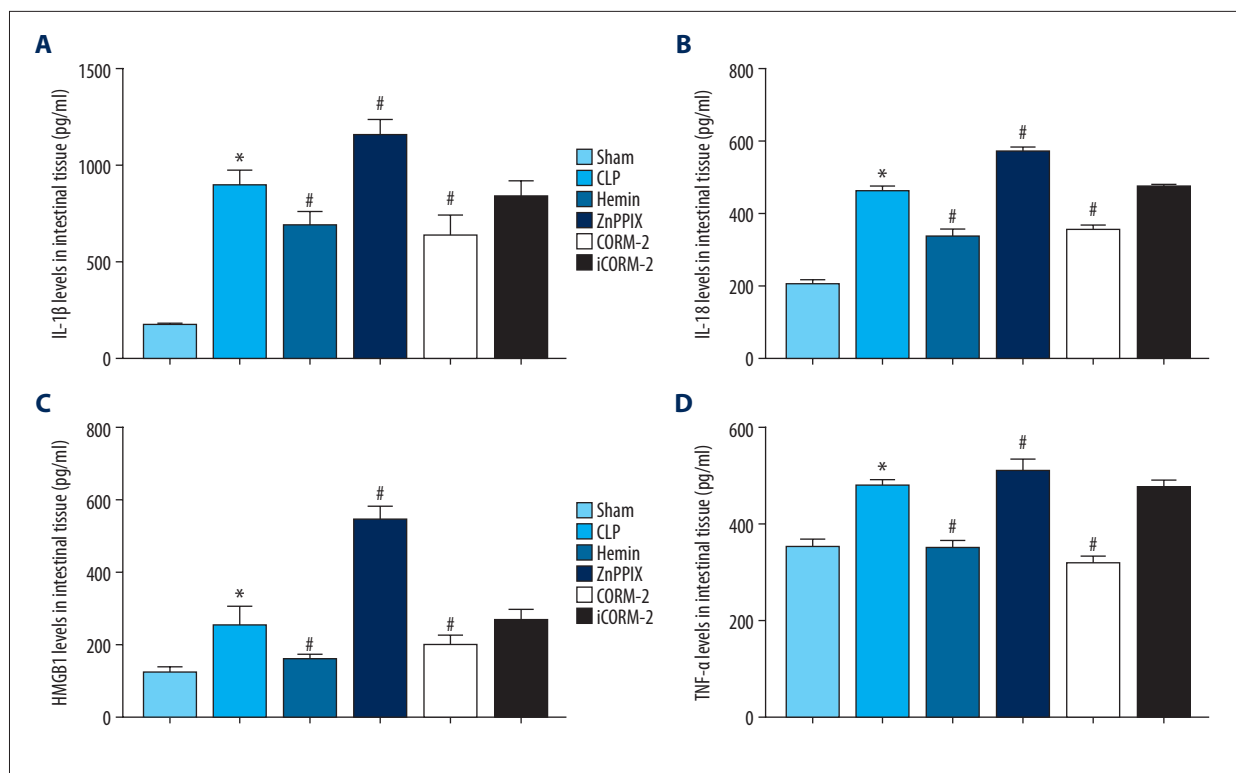


**Figure 5. (A–D)** The intestinal tissue levels of proinflammatory cytokines in the study groups in the rat model of sepsis induced by cecal ligation and puncture (CLP). Male Sprague-Dawley rats (n=120) were divided into six study groups: the sham group, the CLP group, the hemin group (treated with ferric chloride and heme), the zinc protoporphyrin IX (ZnPPIX) group, the CO-releasing molecule 2 (CORM-2) group, and the inactive CORM-2 (iCORM-2) group. The bars represent the mean±standard error (SE) (n=3–5), \* P<0.05 versus the sham group. # P<0.05 versus the CLP group. FD-4 – fluorescein isothiocyanate-labeled dextran 3000–4000 KDa; CLP – cecal ligation and puncture; CORM-2 – CO-releasing molecule 2; Hemin – ferric chloride heme; ZnPPIX – zinc protoporphyrin IX; iCORM-2 – inactive CORM-2.

Pyroptosis is a form of programmed cell death associated with inflammation, which is mainly mediated by caspase-1 and caspase-11 in rat tissue [9,23–25]. Caspase-11 is an inactive precursor, and its active form, caspase-11 p20, is involved in caspase-11-mediated pyroptosis [26]. Increased activation of pyroptosis has a critical role in the occurrence and development of sepsis [10]. Wu et al. showed that intestinal cells might be protected from damage during sepsis by reducing pyroptosis [13]. Zhang et al. reported that CO-releasing molecule 2 (CORM-2) suppressed the activation of the NLRP3 inflammasome in myocardial dysfunction associated with sepsis [14]. Wang et al. showed that CORM-2 reduced the activation of the NLRP3 inflammasome in a rat model of sepsis and that the NLRP3 inflammasome was an important factor in pyroptosis [15]. The findings from the present study showed that CO reduced the inflammatory response and reduced intestinal tissue damage in the CLP rat model of sepsis by reducing pyroptosis of cells in the intestinal mucosa.

In the present study, the role of CO on the expression of proteins associated with intestinal mucosal pyroptosis was

investigated in a rat model of sepsis induced by cecal ligation and puncture (CLP). Male Sprague-Dawley rats were divided into six study groups: the sham group, the CLP group, the hemin group (treated with ferric chloride and heme), the zinc protoporphyrin IX (ZnPPIX) group, the CO-releasing molecule 2 (CORM-2) group, and the inactive CORM-2 (iCORM-2) group. The findings showed that hemin and CORM-2 promoted the survival rate of rats in the CLP-induced sepsis model, which supported the findings from previous studies [27,28]. The findings also showed that hemin and CORM-2 reduced intestinal mucosal damage (Figure 3) and reduced intestinal permeability in rats in the model of sepsis (Figure 2). Also, hemin and CORM-2 reduced the levels of TNF- $\alpha$ , IL-1 $\beta$ , IL-18, and HMGB1 in the serum and intestinal tissue homogenates from rats in the model of sepsis. CO has previously been reported to prevent TNF- $\alpha$ -mediated inflammatory damage through the Akt/Bcl-2 signaling pathway [29], and CO has been reported to inhibit NF- $\kappa$ B activity from downregulating TNF- $\alpha$  expression [29–31]. CO protects against organ injury partly by inhibiting neutrophil aggregation and by reducing TNF- $\alpha$  expression [32]. In the present study, the level of TNF- $\alpha$  was reduced



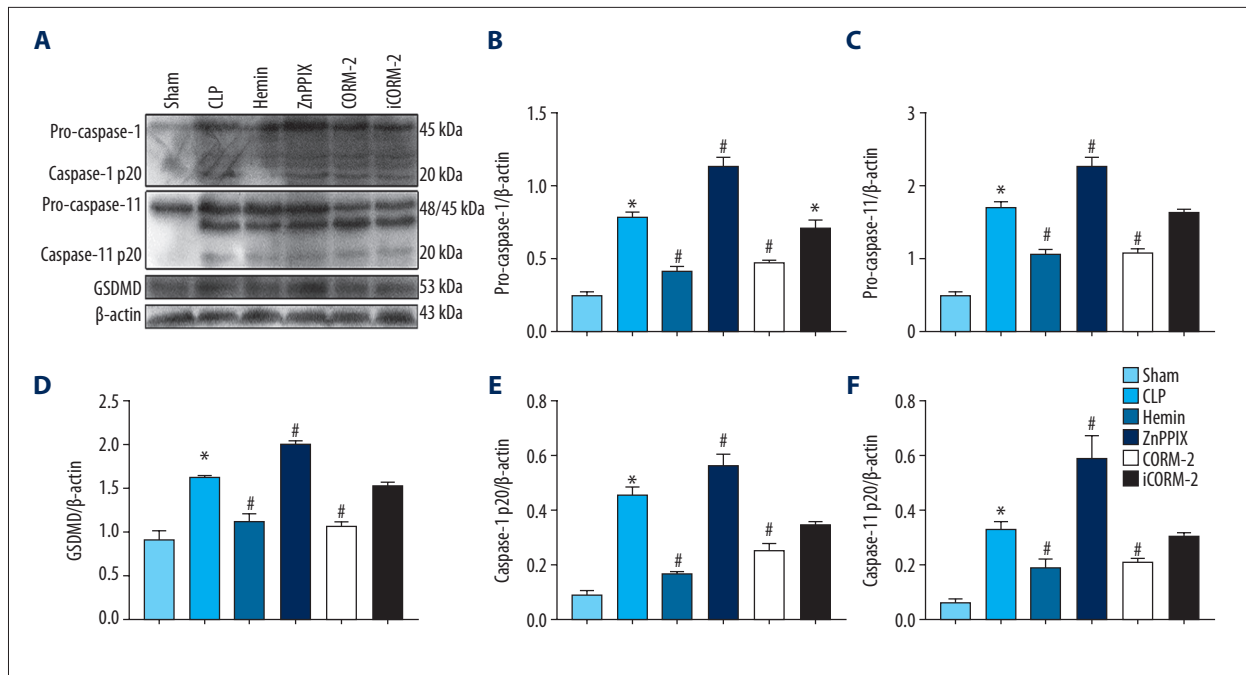


**Figure 6.** The expression of pyroptosis-associated proteins in the study groups in the rat model of sepsis induced by cecal ligation and puncture (CLP). Male Sprague-Dawley rats (n=120) were divided into six study groups: the sham group; the CLP group; the hemin group (treated with ferric chloride and heme); the zinc protoporphyrin IX (ZnPPiX) group; the CO-releasing molecule 2 (CORM-2) group; and the inactive CORM-2 (iCORM-2) group. The expression of pro-caspase-1, pro-caspase-11, caspase-1 p20, caspase-11 p20, and gasdermin D (GSDMD) in the intestinal mucosa. β-actin was used as an internal control. (A) Western blot results for pro-caspase-1, pro-caspase-11, caspase-1 p20, caspase-11 p20, and GSDMD in the intestinal mucosa. (B) The relative level of pro-caspase-1 expression. (C) The relative level of pro-caspase-11 expression. (D) The relative level of GSDMD expression. (E) The relative level of caspase-1 p20 expression. (F) The relative level of caspase-11 p20 expression. The bars represent the mean±SE (n=3-5). \* P<0.05 versus the sham group. # P<0.05 versus the CLP group. CLP – cecal ligation and puncture; CORM-2 – CO-releasing molecule 2; Hemin – ferric chloride heme; ZnPPiX – zinc protoporphyrin IX; iCORM-2 – inactive CORM-2.

in the hemin and CORM-2 groups, which showed that CO had an anti-inflammatory effect.

High mobility group box 1 (HMGB1) is an important late mediator in the development of sepsis [33], and the levels of HMGB1 are increased in tissues during sepsis [34,35]. Antibodies that neutralize HMGB1 may confer protection against tissue damage and injury during endotoxemia, sepsis, and damage to the gut barrier function [36-38]. Previous studies have shown that HMGB1 is a biomarker of pyroptosis that is released during pyroptosis by the regulated classical components of the inflammasome [39,40]. The findings from the present study showed that hemin and CORM-2 reduced the level of HMGB1 in the rat model of sepsis, which is consistent with the anti-inflammatory effect of CO. These results indicated that CO reduced the inflammatory reaction and damage to the intestinal mucosa by preventing the production of HMGB1.

IL-1β is produced as a proprotein, which is proteolytically processed to its active form by caspase-1. IL-1β is an important mediator of the inflammatory response and often amplifies

the effects of other cytokines in a variety of cellular activities [41]. IL-18 is released during pyroptosis and induces further inflammatory reactions and inflammatory disorders. In this study, hemin and CORM-2 reduced the levels of IL-1β and IL-18 in the serum and intestinal mucosa of rats in the model of sepsis, which is consistent with the anti-inflammatory effect of CO. Therefore, these results indicated that CO reduced the inflammatory reaction and intestinal mucosal damage by preventing the production of IL-1β and IL-18.

The results of Western blot and immunofluorescence staining in this study showed that CO reduced the expression of caspase-1, caspase-11, and gasdermin D (GSDMD) in the intestinal mucosa. Following CLP surgery, the inflammatory response increased the expression of caspase-1 and caspase-11. It has previously been reported that when caspase-1 and caspase-11 are cleaved to caspase-1 p20 and caspase-11 p20, respectively, this results in GSDMD cleavage [42]. GSDMD is an effector molecule for pyroptosis, and when GSDMD cleavage cytotoxicity is triggered, and the GSDMD-N-terminal cleavage product localizes to the plasma membrane it forms pores

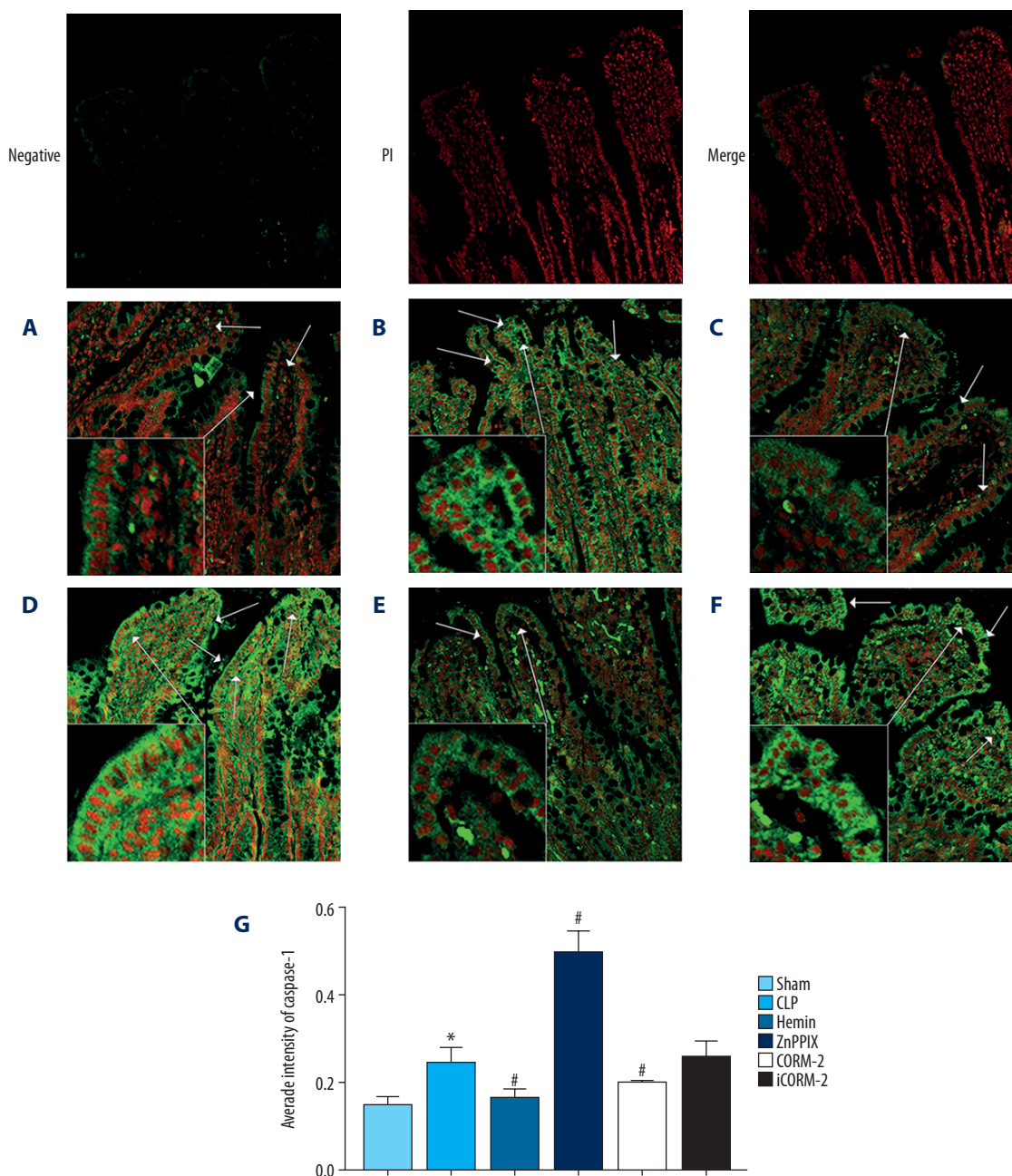


**Figure 7.** Laser confocal microscopy detection of caspase-1 in the intestinal tissue in the study groups in the rat model of sepsis induced by cecal ligation and puncture (CLP). Original magnification,  $\times 200$ . Negative, PI, and merge indicate the negative control group that was incubated without caspase-1 primary antibody and the nucleus stained with propidium iodide (PI). Male Sprague-Dawley rats ( $n=120$ ) were divided into six study groups. (A) The sham group, (B) The CLP group. (C) The hemin group (treated with ferric chloride and heme). (D) The zinc protoporphyrin IX (ZnPPiX) group. (E) The CO-releasing molecule 2 (CORM-2) group. (F) The inactive CORM-2 (iCORM-2) group. (G) The average fluorescence intensity in the study groups. Red presents the nucleus, and green presents caspase-1 protein. The bars represent the mean  $\pm$  SE ( $n=3-5$ ). \*  $P < 0.05$  versus the sham group. #  $P < 0.05$  versus the CLP group. CLP – cecal ligation and puncture; CORM-2 – CO-releasing molecule 2; Hemin – ferric chloride heme; ZnPPiX – zinc protoporphyrin IX; iCORM-2 – inactive CORM-2.

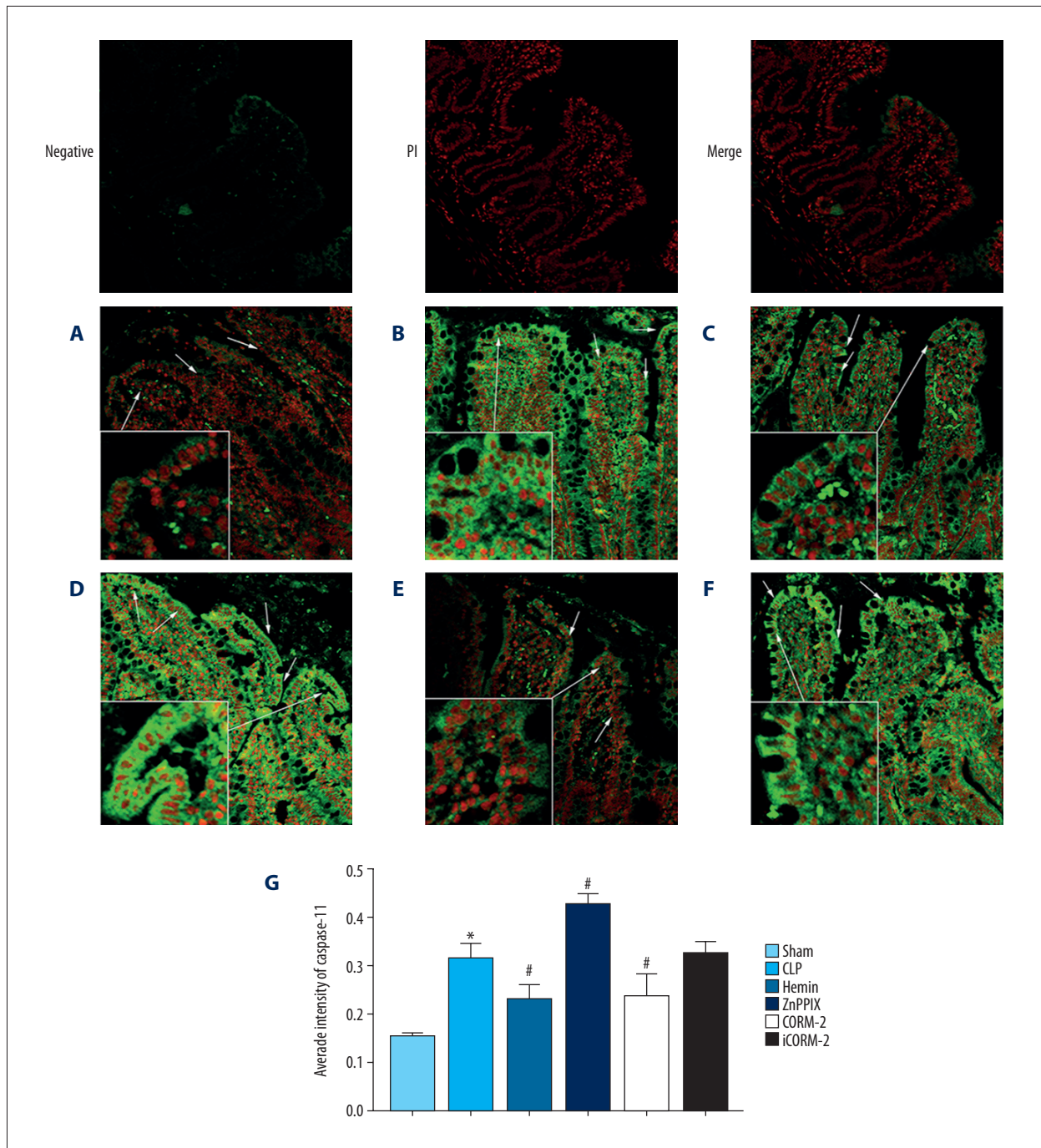


**Figure 8.** Laser confocal microscopy detection of caspase-11 in the intestinal tissue in the study groups in the rat model of sepsis induced by cecal ligation and puncture (CLP). Original magnification,  $\times 200$ . Negative, PI, and merger indicate the negative control group that was incubated without caspase-11 primary antibody and the nucleus stained with propidium iodide (PI). Male Sprague-Dawley rats ( $n=120$ ) were divided into six study groups. (A) The sham group, (B) The CLP group. (C) The hemin group (treated with ferric chloride and heme). (D) The zinc protoporphyrin IX (ZnPPiX) group. (E) The CO-releasing molecule 2 (CORM-2) group. (F) The inactive CORM-2 (iCORM-2) group. (G) The average fluorescence intensity in the study groups. Red presents the nucleus, and green presents caspase-11 protein. The bars represent the mean  $\pm$  SE ( $n=3-5$ ). \*  $P<0.05$  versus the sham group. #  $P<0.05$  versus the CLP group. CLP – cecal ligation and puncture; CORM-2 – CO-releasing molecule 2; Hemin – ferric chloride heme; ZnPPiX – zinc protoporphyrin IX; iCORM-2 – inactive CORM-2.

and promotes the release of IL-1 $\beta$  and IL-18 by active caspase-1 and caspase-11. Also, active caspase-1 and caspase-11 cleave pro-IL-1 $\beta$  and pro-IL-18, and caspase-1 is produced as a zymogen that can be cleaved into 20 kDa (p20) and 10 kDa (p10) subunits, which in turn can cleave the pyroptosis inducer GSDMD [7,42–45]. Hemin and CORM-2 suppress the upregulation of caspase-1, caspase-11, caspase-1 p20, caspase-11 p20, and GSDMD, whereas caspase-1 is activated during pyroptosis by the canonical pyroptosome or caspase-11. The activation of caspase-1 results in GSDMD cleavage (GSDMD-N), to form the membrane pore, which releases inflammatory molecules, including ATP, HMGB1, IL-1 $\beta$ , and IL-18 from the cytosol [46,47]. The production of downstream IL-1 $\beta$  of caspase-11 requires the canonical NLRP3 inflammasome and activated caspase-1 [48]. We found that CO inhibited the expression of pro-caspase-1 and pro-caspase-11, caspase-1 p20 and caspase-11 p20, and GSDMD, which indicated that CO improved the survival rate and reduced intestinal damage by inhibiting the intestinal mucosa pyroptosis-associated proteins. Previous studies have shown that pyroptosis is associated with sepsis, and promotes the rapid clearance of bacterial and viral infection and that CO prevents intestinal inflammation by promoting bacterial clearance [49,50]. However, the mechanisms through which CO indirectly or directly regulates the synthesis and cleavage of pro-caspase-1 and pro-caspase-11 requires further study. GSDMD has been identified as a direct downstream target of caspase-1 and caspase-11 [51,52] and is required for pyroptosis and the involvement of the inflammasome [42,53]. However, the mechanism of CO regulation of GSDMD remains unknown. An increased understanding of the mechanism through which CO acts on pyroptosis may provide a new approach for therapeutic intervention in inflammatory caspase-associated sepsis.

The findings from the present study showed that CO improved the intestinal mucosa by inhibiting pyroptosis in the rat model of CLP-induced sepsis. Previous studies have shown that CO can regulate autophagy or apoptosis to remove pathogenic substances from cells in sepsis or other inflammatory reactions [30]. This study also showed that pyroptosis had a role in the mechanism by which CO acted on the intestinal barrier in the rat model of CLP-induced sepsis. CO regulated the caspase-1 associated canonical and caspase-11 associated non-canonical pathway to inhibit intestinal cell pyroptosis, providing a foundation for future studies of this mechanism. In this study, the effects of CO on intestinal cell pyroptosis was assessed at 24 h in the rat model of sepsis, with individual treatments in the study groups, but a more significant effect may have occurred with multiple drug treatments [53,54].

CORM-2 is a metal complex containing ruthenium, manganese, and molybdenum, which carry CO bound to metals. Therefore, a minimum effective dose was used to avoid metal poisoning. In future studies, assessment of the effects and mechanisms of CO on the control of sepsis should be performed with repeated and multiple drug treatment. The application of CO for the treatment of clinical diseases has been determined extensively in diseases including acute kidney injury, myocardial injury, and sepsis [55–57]. CORM-2 was selected for use in the present study, rather than the clinically used water-soluble CORMs, including CORM-A1 and CORM-3 [58]. There are several potential clinical applications of CO therapy that are under investigation. For example, an extracorporeal CO release system has recently been developed and is used in the treatment of cardiac and respiratory diseases and is used in the application of intensive care applications, including in organ transplantation and sepsis [59].

This study had several limitations. The study was conducted in a rat model, which will show responses that differ from humans. The CLP method was selected for use to represent the human clinical condition, but all animal models are limited in this respect. Pyroptosis-associated proteins and three cytokines, IL-1 $\beta$ , IL-18, HMGB1, were only investigated to represent pyroptosis, mainly due to limited resources and equipment. Future studies should measure additional proteins associated with pyroptosis and explore the relative pathways using specific protein inhibitors or activators. The current study focused on the whole organism and did not assess the effects of sepsis at the cellular level, which is a limitation that should be addressed in future studies.

## Conclusions

This study aimed to investigate the role of carbon monoxide (CO) on the expression of proteins associated with intestinal mucosal pyroptosis in a rat model of sepsis induced by cecal ligation and puncture (CLP). CO had a protective role by inhibiting intestinal mucosal pyroptosis, and by inhibiting the expression of the proinflammatory cytokines, interleukin (IL)-18, IL-1 $\beta$  and high mobility group box protein 1 (HMGB1) and the expression of caspase-1, caspase-11, caspase-1 p20, caspase-11 p20, and gasdermin D (GSDMD). These findings might explain how the effects of CO increased the survival rate of rats in the model of CLP-induced sepsis.

## Conflict of interest

None.

## References:

1. Singer M, Deutschman CS, Seymour CW et al: The Third International Consensus Definitions for Sepsis and Septic Shock (Sepsis-3). *JAMA*, 2016; 315: 775–87
2. Avlan D, Aksöyök S, Salman T et al: The effect of Pentoxifyline on the bacterial translocation and intestinal mucosal changes following burns. *Pediatric Cerrahi Dergisi*, 2002; 16: 121–26
3. Boerma EC, van der Voort PH, Spronk PE, Ince C: Relationship between sublingual and intestinal microcirculatory perfusion in patients with abdominal sepsis. *Crit Care Med*, 2007; 35: 1055–60
4. Coopersmith CM, Stromberg PE, Davis CG et al.: Sepsis from *Pseudomonas aeruginosa* pneumonia decreases intestinal proliferation and induces gut epithelial cell cycle arrest. *Crit Care Med*, 2003; 31: 1630–37
5. Hershberg RM, Mayer LF: Antigen processing and presentation by intestinal epithelial cells – polarity and complexity. *Immunol Today*, 2000; 21: 123–28
6. Zhang S, Zheng S, Wang X et al.: Carbon monoxide-releasing molecule-2 reduces intestinal epithelial tight-junction damage and mortality in septic rats. *PLoS One*, 2015; 10: e0145988
7. Wang J, Sahoo M, Lantier L et al.: Caspase-11-dependent pyroptosis of lung epithelial cells protects from melioidosis while caspase-1 mediates macrophage pyroptosis and production of IL-18. *PLoS Pathogens*, 2018; 14: e1007105
8. Cookson BT, Brennan MA: Proinflammatory programmed cell death. *Mol Microbiol*, 2001; 9: 113–14
9. Bergsbaken T, Fink SL, Cookson BT: Pyroptosis: Host cell death and inflammation. *Nat Rev Microbiol*, 2009; 7: 99–109
10. Chen L, Zhao Y, Lai D et al.: Neutrophil extracellular traps promote macrophage pyroptosis in sepsis. *Cell Death Dis*, 2018; 9: 597
11. Chu LH, Indramohan M, Ratsimandresy RA et al.: The oxidized phospholipid oxPAPC protects from septic shock by targeting the non-canonical inflammasome in macrophages. *Nat Commun*, 2018; 9: 996
12. Jorgensen I, Miao EA: Pyroptotic cell death defends against intracellular pathogens. *Immunol Rev*, 2015; 265: 130–42
13. Wu D, Han R, Deng S et al.: Protective effects of flagellin A/N/C against radiation-induced NLR pyrin domain containing 3 inflammasome-dependent pyroptosis in intestinal cells. *Int J Radiat Oncol Biol Phys*, 2018; 101(1): 107–17
14. Zhang W, Tao A, Lan T et al.: Carbon monoxide releasing molecule-3 improves myocardial function in mice with sepsis by inhibiting NLRP3 inflammasome activation in cardiac fibroblasts. *Basic Res Cardiol*, 2017; 112: 16
15. Wang P, Huang J, Li Y et al.: Exogenous carbon monoxide decreases sepsis-induced acute kidney injury and inhibits NLRP3 inflammasome activation in rats. *Int J Mol Sci*, 2015; 16: 20595–608
16. Chen H, Lu Y, Cao Z et al.: Cadmium induces NLRP3 inflammasome-dependent pyroptosis in vascular endothelial cells. *Toxicol Lett*, 2016; 246: 7–16
17. Chiu CJ, Mcardle AH, Brown R et al.: Intestinal mucosal lesion in low-flow states. I. A morphological, hemodynamic, and metabolic reappraisal. *Arch Surg*, 1970; 101: 478–83
18. Rowlands BJ, Soong CV, Gardiner KR: The gastrointestinal tract as a barrier in sepsis. *Br Med Bull*, 1999; 55: 196–211
19. Macfie J, O’Boyle C, Mitchell CJ et al.: Gut origin of sepsis: A prospective study investigating associations between bacterial translocation, gastric microflora, and septic morbidity. *Gut*, 1999; 45: 223–28
20. Perez-Chanona E, Mühlbauer M, Jobin C: The microbiota protects against ischemia/reperfusion-induced intestinal injury through nucleotide-binding oligomerization domain-containing protein 2 (NOD2) signaling. *Am J Pathol*, 2014; 184(11): 2965–75
21. Liu W, Wang XH, Yang XJ et al.: [Intestinal barrier dysfunction and its related factors in patients with sepsis.] *Zhonghua Yi Xue Za Zhi*, 2016; 96: 3568–72 [in Chinese]
22. Yoseph BP, Klingensmith NJ, Liang Z et al.: Mechanisms of intestinal barrier dysfunction in sepsis. *Shock*, 2016; 46: 52–59
23. Fink SL, Cookson BT: Caspase-1-dependent pore formation during pyroptosis leads to osmotic lysis of infected host macrophages. *Cellular Microbiol*, 2006; 8: 1812–25
24. Hagar JA, Powell DA, Aachoui Y et al.: Cytoplasmic LPS activates caspase-11: implications in TLR4-independent endotoxemic shock. *Science*, 2013; 341: 1250–53
25. Kayagaki N, Wong MT, Stowe IB et al.: Noncanonical inflammasome activation by intracellular LPS independent of TLR4. *Science*, 2013; 341: 1246–49
26. Petr B, Monack DM: Noncanonical inflammasomes: Caspase-11 activation and effector mechanisms. *PLoS Pathogens*, 2013; 9: e1003144
27. Lee S, Lee SJ, Coronata AA et al.: Carbon monoxide confers protection in sepsis by enhancing beclin 1-dependent autophagy and phagocytosis. *Antioxid Redox Signal*, 2014; 20(3): 432–42
28. Lancel S, Hassoun SM, Favory R et al.: Carbon monoxide rescues mice from lethal sepsis by supporting mitochondrial energetic metabolism and activating mitochondrial biogenesis. *J Pharmacol Exp Ther*. 2009; 329(2): 641–48
29. Basuroy S, Bhattacharya S, Leffler CW, Parfenova H: Nox4 NADPH oxidase mediates oxidative stress and apoptosis caused by TNF-alpha in cerebral vascular endothelial cells. *Am J Physiol Cell Physiol*, 2009; 296(3): C422–32
30. Wang X, Cao J, Sun BW et al.: Exogenous carbon monoxide attenuates inflammatory responses in the small intestine of septic mice. *World J Gastroenterol*, 2012; 18: 5719–28
31. Zhang P, Zou XQ, Shi GS, Sun BW: [Inhibition effects of carbon monoxide-releasing molecules-2 to lung inflammatory in sepsis mice.] *Journal of Jiangsu University*, 2010; 2 [in Chinese]
32. Han N, Chen WM: [Effects of exogenous carbon monoxide on polymorphonuclear neutrophil, TNF-alpha and IL-10 expression in rats with intestinal ischemia reperfusion injury.] *World Chinese Journal of Digestology*, 2009; 17: 74 [in Chinese]
33. Wang H, Ward MF, Sama AE: Novel HMGB1-inhibiting therapeutic agents for experimental sepsis. *Shock*, 2009; 32(4): 348–57
34. Yang H, Wang H, Chavan SS, Andersson U: High mobility group box protein 1 (HMGB1): The prototypical endogenous danger molecule. *Mol Med*, 2015; 21(Suppl. 1): S6–12
35. Magna M, Pisetsky DS.: The role of HMGB1 in the pathogenesis of inflammation and autoimmune diseases. *Mol Med*, 2014; 20: 138–46
36. Kobayashi M, Tamari K, Salihi MOA et al.: Anti-high mobility group box 1 antibody suppresses local inflammatory reaction and facilitates olfactory nerve recovery following injury. *J Neuroinflamm*, 2018; 15: 124
37. Yang R, Harada T, Mollen KP et al.: Anti-HMGB1 neutralizing antibody ameliorates gut barrier dysfunction and improves survival after hemorrhagic shock. *Mol Med*, 2006; 12: 105–14
38. Nishibori M: [HMGB1 as a representative DAMP and anti-HMGB1 antibody therapy]. *Nihon Yakurigaku Zasshi*, 2018; 151(1): 4–8 [in Japanese]
39. Van ON, Gurung P, Vande WL et al.: Activation of the NLRP1b inflammasome independently of ASC-mediated caspase-1 autoproteolysis and speck formation. *Nat Commun*, 2014; 5: 3209
40. Hou L, Yang Z, Wang Z et al.: NLRP3/ASC-mediated alveolar macrophage pyroptosis enhances HMGB1 secretion in acute lung injury induced by cardiopulmonary bypass. *Lab Invest*, 2018; 98(8): 1052–64
41. Mridha AR, Wree A, Aab R et al.: NLRP3 inflammasome blockade reduces liver inflammation and fibrosis in experimental NASH in mice. *J Hepatol*, 2017; 66: 1037–46
42. Shi J, Zhao Y, Wang K et al.: Cleavage of GSDMD by inflammatory caspases determines pyroptotic cell death. *Nature*, 2015; 526: 660–65
43. Xu B, Jiang M, Chu Y et al.: Gasdermin D plays a key role as a pyroptosis executor of non-alcoholic steatohepatitis in humans and mice. *J Hepatol*, 2018; 68(4): 773–82
44. Sahoo M, Barrio L, Miller MA, Re F: Role of elastase in IL-1 $\beta$  and IL-18 processing and pyroptosis. *PLoS Pathog*, 2014; 10(8): e1004327
45. Kuang S, Zheng J, Yang H et al.: Structure insight of GSDMD reveals the basis of GSDMD autoinhibition in cell pyroptosis. *Proc Natl Acad Sci USA*, 2017; 114: 10642–47
46. Fernandes-Alnemri T, Wu J, Yu JW et al.: The pyroptosome: a supramolecular assembly of ASC dimers mediating inflammatory cell death via caspase-1 activation. *Cell Death Differ*, 2007; 14(9): 1590–604
47. Kang SJ, Wang S, Hara H et al.: Dual role of caspase-11 in mediating activation of caspase-1 and caspase-3 under pathological conditions. *J Cell Biol*, 2000; 149(3): 613–22
48. Aachoui Y, Sagulenko V, Miao EA, Stacey KJ: Inflammasome-mediated pyroptotic and apoptotic cell death, and defense against infection. *Curr Opin Microbiol*, 2013; 16(3): 319–26

49. Miao EA, Leaf IA, Treuting PM et al: Caspase-1-induced pyroptosis is an innate immune effector mechanism against intracellular bacteria. *Nat Immunol*, 2010; 11: 1136–42
50. Casson CN, Copenhaver AM, Zwack EE et al: Caspase-11 activation in response to bacterial secretion systems that access the host cytosol. *PLoS Pathogens*, 2013; 9: e1003400
51. Sborgi L, Rühl S, Mulvihill E et al: GSDMD membrane pore formation constitutes the mechanism of pyroptotic cell death. *EMBO J*, 2016; 35: 1766–78
52. Xing L, Zhang Z, Ruan J et al: Inflammasome – activated gasdermin D causes pyroptosis by forming membrane pores. *Nature*, 2016; 535: 153–58
53. Kayagaki N, Stowe IB, Lee BL et al: Caspase-11 cleaves gasdermin D for non-canonical inflammasome signaling. *Nature*, 2015; 526: 666–71
54. Zhou Z, Shuang MA, Liu J et al: Protective effects of endogenous carbon monoxide against myocardial ischemia-reperfusion injury in rats. *Acta Physiologica Sinica*, 2018; 70(2): 115–22
55. Nakao A, Yamada T, Kohama K et al: Application of carbon monoxide for treatment of acute kidney injury. *Acute Med Surg*, 2014; 1(3): 127–34
56. Nakahira K, Choi AM: Carbon monoxide in the treatment of sepsis. *Am J Physiol Lung Cell Mol Physiol*, 2015; 309: 1387–93
57. Segersvärd H, Lakkisto P, Hänninen M et al: Carbon monoxide releasing molecule improves structural and functional cardiac recovery after myocardial injury. *Eur J Pharmacol*, 2017; 818: 57–66
58. Ling K, Men F, Wang WC et al: Carbon monoxide and its controlled release-therapeutic application, detection and development of carbon monoxide-releasing molecules (CO-RMs). *J Med Chem*, 2017; 61: 2611–35
59. Wollborn J, Hermann C, Goebel U et al: Overcoming safety challenges in CO therapy - Extracorporeal CO delivery under precise feedback control of systemic carboxyhemoglobin levels. *J Control Release*, 2018; 279: 336–44